# Biogeography-based Optimized Adaptive Neuro-Fuzzy Control of a Nonlinear Active Suspension System

Ali Fayazi[1*], Hossein Ghayoumi Zadeh[2]
1- Department of Electrical Engineering, Vali-e-Asr University of Rafsanjan, Rafsanjan, Iran.
Email: a.fayazi@vru.ac.ir (Corresponding author)
2- Department of Electrical Engineering, Vali-e-Asr University of Rafsanjan, Rafsanjan, Iran.
Email: h.ghayoumizadeh@vru.ac.ir

Received: November 2021 Revised: December 2021 Accepted: February 2022

**ABSTRACT:**
This paper presents an optimum network structure based on a BBO tuned adaptive neuro-fuzzy inference system (ANFIS) to control an active suspension system (ASS). The unsupervised learning via Biogeography-Based Optimization (BBO) algorithm is used to train the ANFIS network. The optimal proportional-integral-derivative controller tuned based on the LQR method is used to generate the training data set. ANFIS base on Fuzzy c-means (FCM) clustering algorithm is applied to approximate the relationships between the vehicle body (sprung mass) vertical input velocity and the actuator output force. BBO algorithm is used to optimize fuzzy c means clustering parameters. The numerical simulation results showed that the proposed optimized BBO-FCMANFIS based vehicle suspension system has better performance as compared with the optimal LQR-PID controller under uncertainties in both of reducing actuator energy consumption and the suppression of the vibration of the sprung mass acceleration, with a 43% and 9.5% reduction, respectively.

**KEYWORDS:** Active Suspension System, Optimal Vibration Control, Biogeography-Based Optimization, Fuzzy c-means clustering, ANFIS

## 1. INTRODUCTION

Modern suspension system is one of the fundamental components of automotive vehicles. The main task of vehicle suspension system (VSS) is to provide passengers' comfort by separating passenger and vehicular body interactions from oscillations caused by road irregularities while still keeping continuous wheel-road contact under any condition to maximize traction. In general, the three most common types of suspension system are: passive suspension systems which is also called conventional lumped mass-spring-damper system [1], semi-active [2], and active suspension systems [2] and [3]. In recent decades, ASS has attracted the interest of the scientific community because of their advantages over the traditional passive suspension systems. The adaptation potential of suspension characteristics in the face of road unevenness is the main important benefit of using an ASS [5]. The main component of an ASS that distinguishes it from the conventional passive suspension system is the use of an active element called actuator which is connected in parallel with the spring and damper to exert a desired force between the vehicle body (sprung mass) and wheel and suspension assembly (unsprung mass). The vehicle control unit is used to determine the desired force for controlling the dynamic behavior of suspension system in order to adapt to road profile, surpass the vibration of sprung mass acceleration and thus to achieve riding comfort.

Over the past decades, various control strategies have suggested to improve the vehicle suspension [6], [7], [8], [9], [10], [11], [12], [13], [14], [15], [16], [17], [18] and [19]. In [6], a robust control scheme based on FOFPD controller is presented for uncertain and nonlinear ASS. In [8], fuzzy fault-tolerant $H^{\infty}$ control scheme is proposed for nonlinear ASS. Some have provided an adaptive backstepping-based tracking control scheme for nonlinear ASS [13] and [18]. In [11], a hybrid ANFIS PID approach is proposed for modeling and control of ASS. Some have proposed a linear fuzzy logic control method combined with genetic algorithm optimization for a half-car model of ASS [19], [20]. In [21], a back stepping method is presented for ASS. In [22] and [23], the authors used a sliding mode control (SMC) method for VASS. In [24] and [25], a FSMC controller is designed to control the VSS. In [26], a neural network based SMC is proposed for VASS. In [27], vehicle body vertical acceleration is



Paper type: Research paper
DOI: https://doi.org/10.52547/mjtd.11.1.43
How to cite this paper: A. Fayazi and H. Ghayoumi Zadeh, "**Biogeography-based Optimized Adaptive Neuro-Fuzzy Control of a Nonlinear Active Suspension System**", Majlesi Journal of Telecommunication Devices, Vol. 11, No. 1, pp. 43-53, 2022.

minimized by fuzzy logic control scheme. In [28], a novel robust neural network control system is presented for vibration control of VASS. In [29], a deep learning structure is designed to control an ASS. Intelligent control is a new interesting area that has recently made significant advances in computing technology. ANFIS control is one of the most important of intelligent control approaches which is a combination of the characteristics of an artificial neural network and the FLC technique.

The neuro-fuzzy system is a powerful tool which has been widely employed in various fields of engineering and medical sciences [30]. It has been shown that neuro-fuzzy controllers can also enhance the performance of ASS [31] and [34]. The conventional neuro-fuzzy methods utilizes the learning algorithms such as the backpropagation algorithm to determine the best values for parameters in fuzzy logic system [28] and [29]. However, the performance of the neuro-fuzzy system can be enhanced by the meta-heuristic method. In this paper, an optimum network structure is presented based on a BBO tuned ANFIS to control an ASS. The ANFIS network was trained by the BBO unsupervised learning algorithm. The full replacement of the traditional optimal LQR-PID controller with a BBO tuned ANFIS controller is the main contribution of this article. A BBO tuned ANFIS control is rarely utilized on its own in the control of ASS as presented here. Simulation results show the effectiveness of the proposed optimized BBO-FCMANFIS controller over the optimal LQR-PID controller under uncertainties in terms of improving actuator power consumption and the suppression of the vibration of the sprung mass acceleration, and as a result riding comfort. The main objectives of the present work are as follows:

i. Design an optimum network structure based on a BBO tuned ANFIS system to improve the performance of a nonlinear ASS.
ii. Full replacement of the traditional optimal LQR-PID controller with a BBO tuned ANFIS controller.
iii. Comparison of the effectiveness of the proposed optimized BBO-FCMANFIS method with the conventional optimal LQR-PID controller under road disturbance and parameters' uncertainties.

The rest of this paper is structured as follows: The material and method is addressed in Section 2. The proposed optimized BBO-FCMANFIS method is introduced in Section 3. Simulation results are provided in Section 4. Eventually, the conclusions are given in Section 5.

## 2. MATERIAL AND METHOD

### 2.1. Quarter car modelling

This section presents a dynamic model of a nonlinear ASS. The dynamic vehicle model is a two Degree Of Freedom (DOF) quarter-car (QC) of ASS. It is a double mass-spring-damper system consists of two masses (sprung and unsprung mass) which is coupled to each other via a spring and a damper as depicted in Fig. 1.

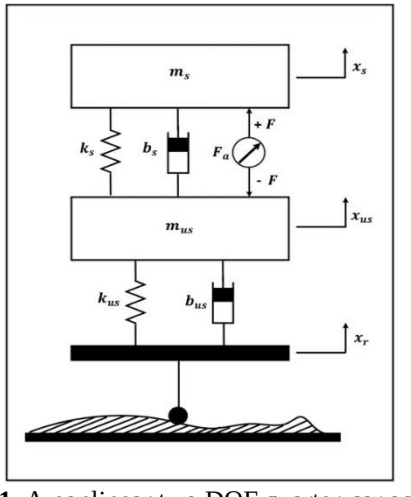


**Fig. 1.** A nonlinear two DOF quarter-car active suspension model.

The following assumptions are made for a nonlinear QC model:
Assumption 1: A nonlinear spring-damper system model is considered for the suspension system.
Assumption 2: There will be no rotational motion in the wheel and the body.
Assumption 3: The dynamic behavior of the spring-damper model is nonlinear.
Assumption 4: The tire and road surface are always in contact and the effect of friction is considered as a linear damper in the vehicle active suspension modeling.

The dynamic equations of a nonlinear two DOF QC model of ASS are given as follows [35]:

$$m_s\ddot{x}_s + b_s sign(\dot{x}_s - \dot{x}_{us})\,|\,\dot{x}_s - \dot{x}_{us}\,|^p + k_s(x_s - x_{us}) = F_a \tag{1}$$
$$m_{us}\ddot{x}_{us} + b_s sign(\dot{x}_{us} - \dot{x}_s)\,|\,\dot{x}_{us} - \dot{x}_s\,|^p + k_s(x_{us} - x_s) + b_{us}(\dot{x}_{us} - \dot{x}_r) + k_{us}(x_{us} - x_r) = -F_a$$

where $m_s$ represents the sprung mass, $m_{us}$ represents the unsprung mass, $k_s$ and $b_s$ are the spring stiffness and damping coefficient of damper of ASS, respectively. $k_{us}$ and $b_{us}$ represent tyre stiffness and

tyre damping coefficient, respectively. $F_a$ represents the actuator force which it is exerted to sprung mass and unsprung mass, $p > 0$ represents the nonlinear damping force index (see [36]). The common linear form of damping force is obtained by setting $p = 1$.

By choosing the state vector as $x(t) = [x_s(t) - x_{us}(t)\ \dot{x}_s(t)\ x_{us}(t) - x_r(t)\ x_{us}(t)]^T$ the state-space representation of nonlinear QC model is given by:

$$
\begin{aligned}
\dot{x}_1(t) &= x_3(t) - x_4(t) \\
\dot{x}_2(t) &= -\frac{k_s}{m_s} x_1(t) - \frac{b_s}{m_s} sign(x_4(t) - x_2(t)) \,|\, x_4(t) - x_2(t) \,|^p + \frac{1}{m_s} F_a \\
\dot{x}_3(t) &= x_4(t) - \dot{x}_r(t) \\
\dot{x}_4(t) &= \frac{k_s}{m_{us}} x_1(t) + \frac{b_s}{m_{us}} sign(x_4(t) - x_2(t)) \,|\, x_4(t) - x_2(t) \,|^p - \frac{k_{us}}{m_{us}} x_3(t) - \frac{b_{us}}{m_{us}} x_4(t) + \frac{b_{us}}{m_{us}} \dot{x}_r(t) - \frac{1}{m_{us}} F_a \\
y_1(t) &= x_1(t) = x_s(t) - x_{us}(t) \\
y_2(t) &= -\frac{k_s}{m_s} x_1(t) - \frac{b_s}{m_s} sign(x_4(t) - x_2(t)) \,|\, x_4(t) - x_2(t) \,|^p + \frac{1}{m_s} F_a = \ddot{x}_s(t)
\end{aligned}
\tag{2}
$$

where $x_1$ is the vertical deflection of suspension system $(x_s - x_{us})$, $x_2$ is the vertical velocity of sprung mass $\dot{x}_s$ , $x_2$ is the wheel displacement $(x_{us} - x_r)$, and $x_4$ is the vertical velocity of the wheel $\dot{x}_{us}$. The actuator force $F_a$ is the control input signal $u$ and $\dot{x}_r$ represents the external disturbance input. The first output of ASS is the suspension deflection $(x_s - x_{us})$, and the second output of ASS is the vehicle body acceleration $\ddot{x}_s$. The parameters of the QC model are given in Table 1.

**Table 1.** Physical parameters of suspension system.

| Parameter | Description | Value |
|---|---|---|
| $m_s$ | Sprung mass | 2.45 (kg) |
| $m_{us}$ | Unsprung mass | 1 (kg) |
| $k_s$ | Stiffness of the car suspension | 900 (N/m) |
| $k_{us}$ | Stiffness of the tyre | 2500 (N/m) |
| $b_s$ | Suspension damping coefficient | 7.5 (Ns/m) |
| $b_{us}$ | Tyre damping coefficient | 1 (Ns/m) |
| p | Nonlinear damping force index | 3 |

### 2.2. Passive Suspension System

The passive suspension system can be considered as the open loop response of the system by choosing $F_a = 0$ in (2). In this situation, the suspension system receives no control signal from the actuator.

### 2.3. Active Suspension System

The passive suspension system can be turned to an active suspension includes an actuator that can supply active force regulated by an optimal PID controller algorithm [37]. In this control scheme, two QC suspension parameters namely the vertical deflection of suspension system $(x_s - x_{us})$ and the sprung mass vertical velocity $\dot{x}_s$ are fedback to the controllers to reduce the impact of road irregularities. The block diagram representation of control is shown in Fig. 2.

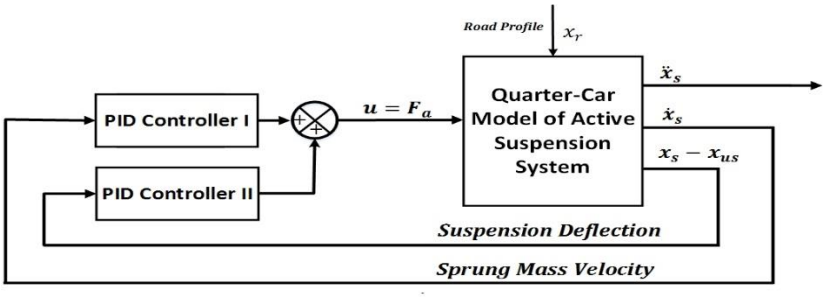


**Fig. 2.** Closed-loop control system of ASS.

To achieve the best robust performance for both PID controllers, Auto tuning has been accomplished by using the MATLAB simulation software. The optimum gain values of the PID controllers are given in Table 2..

**Table 2.** Tuned gain values of PID controllers

| Controller | $K_P$ | $K_I$ | $K_D$ |
|---|---|---|---|
| PID Controller I | 100.9862 | 0.5621 | 0.0163 |
| PID Controller II | 100.9862 | 0.4137 | 0.0030 |

## 3. BBO TUNED ANFIS

### 3.1. Training of ANFIS

Training, testing, and validation are the three main stages of training procedure. In this work, we used a random portions of the same data to generate the training and testing data. Thus, we used 70% of the data set for training and hold out 30% of the data set for testing. Data set using an actual road profile were used for validation. In this paper, a training data set is used to create an initial fuzzy inference system (FIS) in which, the hybrid optimization algorithm has been used to adjust membership functions. The aforementioned closed loop optimal PID controller scheme is used to achieve the training data. Data collection is generated by considering a double mass-spring-damper system as a QC model of ASS in the face of a random road profile excitation. The actuator force $F_a$ is employed as target data while suspension deflection $(x_s - x_{us})$ and sprung mass vertical velocity $\dot{x}_s$ are used as input variables data to the ANFIS. In this paper, the following first order Sugeno model fuzzy inference with two inputs is used for ANFIS:

$Rule_i$: If suspension deflection is $A_i$ and sprung mass velocity is $B_i$, then $u = f(x_s - x_{us},\ \dot{x}_s)$.

### 3.2. Adaptive Neuro-Fuzzy Inference controller

The adaption potential of ANFIS makes it suitable for learning control. ANFIS has been employed in various fields of science and it has good capability and effectiveness in system identification, state estimation, and control. In this work, an optimized BBO tuned ANFIS model is used to control an ASS. The training data sets are: the actuator force signal, the suspension displacement, and the sprung mass vertical velocity data points per millisecond. The training data set was used to train the ANFIS for modeling the dynamic behavior of the optimal PID controller. Thus, the ultimate goal is that the ANFIS will be able to estimate the appropriate actuator force signal to minimize the sprung mass vertical acceleration under unknown road unevenness. The proposed optimized BBO-FCMANFIS controller scheme is depicted in Fig. 3.

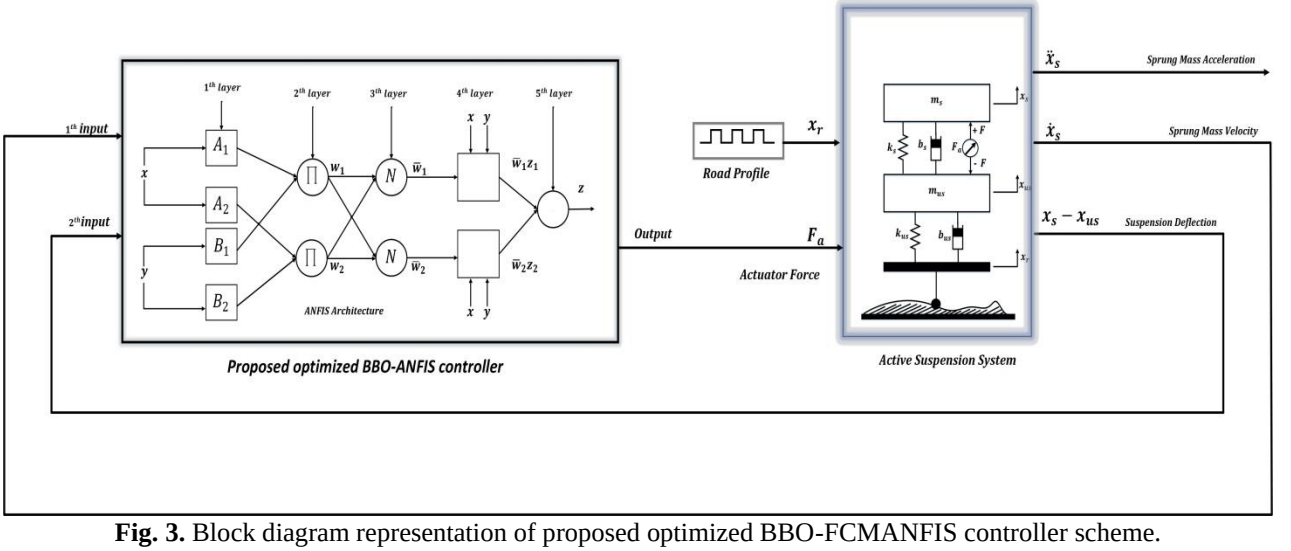


**Fig. 3.** Block diagram representation of proposed optimized BBO-FCMANFIS controller scheme.

The proposed optimized BBO-FCMANFIS controller is shown in Fig. 3. A typical architecture of ANFIS is depicted in Fig. 4. As can be seen from Fig. 4, the ANFIS structure has two inputs (the suspension deflection and the sprung mass velocity) and one output (the actuator force signal). Moreover, the ANFIS has five layers which is detailed in [32] . For a first order Sugeno fuzzy inference model, a typical rule set with two fuzzy IF-THEN rules of Takagi and Sugeno's type is as follows:

Rule $_1$: If $x$ is $A_1$ and $y$ is $B_1$, then $f_1 = p_1x + q_1y + r_1$

Rule $_2$: If $x$ is $A_2$ and $y$ is $B_2$, then $f_2 = p_2x + q_2y + r_2$

Where $A_i$ and $B_i$ are the antecedent part in the fuzzy sets and $f_i$ is the consequent part in the fuzzy sets. $p_i$, $q_i$ and $r_i$ are the node outputs of the updated linear consequent parameters.

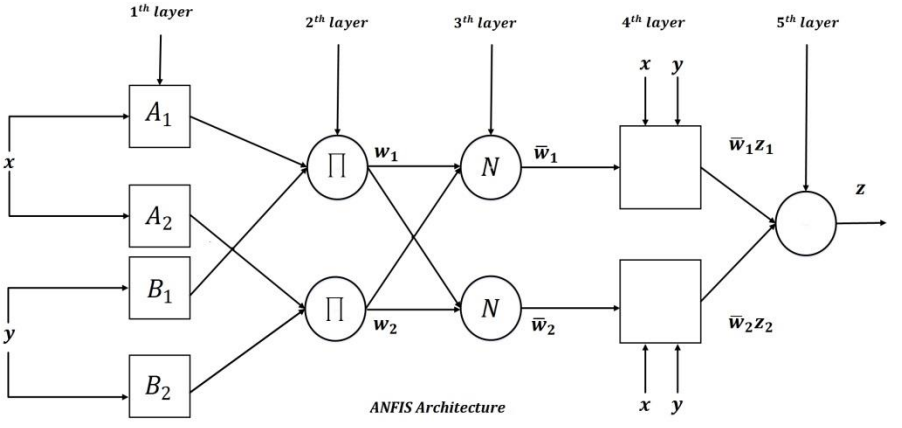


**Fig. 4.** ANFIS architecture.

### 3.3. Fuzzy c-means clustering algorithm

In this section, fuzzy c-means (FCM) clustering method is used to formulate an ANFIS. FCM algorithm is a technique of clustering in which each data point can belong to more than one cluster through varying degrees of membership from 0 to 100 percent. Allowing gradual memberships is the main advantage of FCM clustering in which it provides the opportunity to deal with data points that belong to multiple clusters at the same time. This method is frequently used in pattern recognition applications. In FCM clustering method the aim is to minimize the following objective function:

$$J_m = \sum_{i=1}^{N}\sum_{j=1}^{C} u_{ij}^{m} \left\| x_i - c_j \right\|^2, \; 1 < m < \infty \tag{3}$$

where the number of data points is determined by N, the number of clusters is represented by C, fuzzy partition matrix exponent is determined by m which is used to control the degree of fuzzy overlap and it must be greater than 1. The degree of membership of $x_i$ in the cluster m is determined by $u_{ij}$, $x_i$ represents the $i^{th}$ data point, the center of the $j^{th}$ cluster is indicated by $c_j$, and the similarity between any measured data and the center is determined by $\|*\|$ which can be defined by any norm expressing. An iterative optimization of the above objective function is employed for fuzzy partitioning in which the update of membership $u_{ij}$ and the cluster centers $c_j$ are as follows:

$$u_{ij} = \frac{1}{\sum_{k=1}^{C}\left(\frac{\left\| x_i - c_j \right\|}{\left\| x_i - c_k \right\|}\right)^{\frac{2}{m-1}}}, \; c_j = \frac{\sum_{i=1}^{N} u_{ij}^{m} x_i}{\sum_{i=1}^{N} u_{ij}^{m}} \tag{4}$$

This iteration will stop when $max_{ij}\left(\left|u_{ij}^{(k+1)} - u_{ij}^{(k)}\right|\right) < \epsilon$ where $\epsilon$ represents a termination criterion between 0 and 1 to stop the iterative process and $k$ represent the iteration step . The algorithm consists of the following steps:

Step 1: Randomly initialize the cluster membership values (initialize $U = [u_{ij}]$ matrix, $U^{(0)}$).

Step 2: At $k - step$: Calculate the cluster centers: $C^{(k)} = [c_j]$ with $u^{(k)}$ $c_j = \frac{\sum_{i=1}^{N} u_{ij}^{m} x_i}{\sum_{i=1}^{N} u_{ij}^{m}}$.

Step 3: Update $U^{(k)}$ and $U^{(k+1)}$ according to the following:

$$u_{ij} = \frac{1}{\sum_{k=1}^{C}\left(\frac{\|x_i - c_j\|}{\|x_i - c_k\|}\right)^{\frac{2}{m-1}}}$$

Step 4: Calculate the $J_m$.

Step 5: Repeat steps $2-4$ until $J_m$ reaches a specified maximum number of iterations.

### 3.4. BBO tuning of FCM-ANFIS

In this section, the BBO tuning of the ANFIS parameters is explained. The antecedent and the consequent parameters are two parameter types of the ANFIS structure that have to be tuned. The Gaussian function is chosen for membership functions which it is given by (5):

$$u_{Ai(x)} = \exp\left\{-\left[\left(\frac{x-c_i}{a_i}\right)^2\right]^{b_i}\right\} \quad (5)$$

where $c_i$ represents the centers of membership functions, i. e. mean ($\mu$), $a_i$ is the standard deviation ($\sigma$), and $b_i$ is a tunable parameter. The antecedent parameters of membership functions are illustrated by ($a_i$,$b_i$,$c_i$) while the consequent parameters are illustrated by ($p_i$,$q_i$,$r_i$). The process of fuzzy modeling of the system has been accomplished by the identification of the FIS parameters to estimate a suitable form of the dynamics behavior of the system. The parameters of Gaussian membership functions are central value $c$ and the width $\sigma$. After the primary structure is determined for the fuzzy system, then, the center of every membership function $c$, is tuned by the BBO. The standard deviation of the Gaussian membership function $\sigma$ was specified by the learning algorithm. As consequence, to achieve the best fuzzy model, the parameters of membership function are optimized over the BBO algorithm. The optimal FIS will be obtained by considering the following root mean squared error (RMSE) as an objective function:

$$J(i) = \sqrt{\sum_{j=1}^{p} \frac{1}{p}\left(z_t^j - z_{out}^j\right)^2} \quad (6)$$

where $p$ is the total number of the samples, $z_t^j$ and $z_{out}^j$ are the target output and the predicted model output of $j^{th}$ sample, respectively. $J(i)$ denotes the fitness value of $i^{th}$ individual.

### 3.5. Biogeography-based optimization algorithm

BBO technique is an evolutionary algorithm (EA) that was introduced by Dan Simon for the first time [38]. BBO algorithm optimizes a function by stochastically and iteratively trying to improve candidate solutions. The algorithm is founded based on the phenomenon of migration of animals to different habitats. In general, habitats that are suitable sites for geographical species have high habitat suitability index (HSI). This index is determined by the housing variables called suitability index variables (SIVs). Therefore, HSI is a function of SIVs. the immigration and emigration rate are respectively $\lambda$ and $\mu$ which are determined by the number of species in a habitat (or HSI). High HSI habitat resembles feasible solution while, solution degrades with low HSI habitat. The biological diversity of the population is increased by application of mutation in BBO. The immigration $\lambda$ and emigration rate ($\mu$) are given by (7) and (8), respectively.

$$\lambda_i = I\left(1 - \frac{k(i)}{n}\right) \quad (7)$$

$$\mu_i = E\left(\frac{k(i)}{n}\right) \quad (8)$$

where $I$ and $E$ are respectively the highest rates of immigration ($\lambda$) and emigration rate ($\mu$) that responses can get. $k(i)$ represents the number of species for the $i^{th}$ habitat which is between 1 and $n$. $n$ represents the maximum number of species that the habitat can support. For a condition, where $E = I = 1$ , we have

$$\lambda_i + \mu_i = 1 \quad (9)$$

The flowchart of BBO is depicted in Fig. 5.

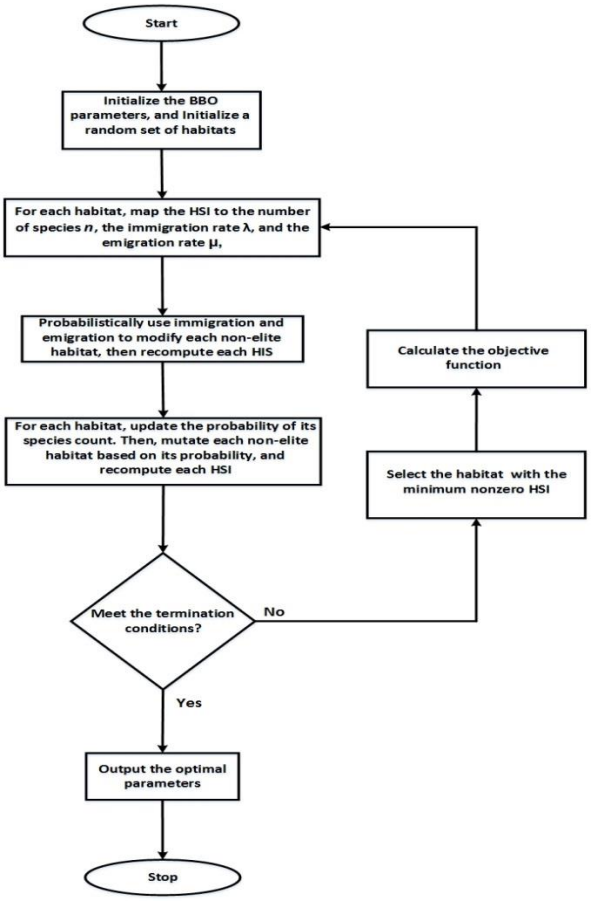


**Fig. 5.** Flowchart of the BBO algorithm.

## 4. SIMULATION RESULTS

Simulations are carried out using SIMULINK/MATLAB R2016a. ANFIS controller is a function of suspension deflection ($x_s - x_{us}$) and sprung mass vertical velocity $\dot{x}_s$. The main parameters of BBO algorithm are chosen as follows: $Pop.\ Size = 50$, $Max.Iter.No = 250$, $Keep\ Rate = 0.2$ , and

$Init.Mut.Prob. = 0.1$. BBO algorithm was used to adjust the parameters of ANFIS by using FCM clustering method. The convergence of cost function is shown in Fig. 6.

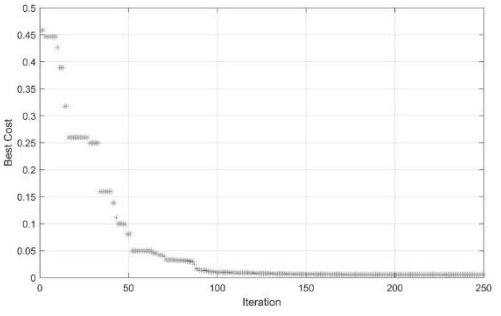


**Fig. 6.** Convergence rate of the BBO algorithm.

The road profile is set to a 3 $(Hz)$ square waveform of $0.02\,(m)$ amplitude for simulating worst case scenario. The road profile is applied to the QC model of ASS. Simulations are accomplished for ASS, ASS with BBO tuned FCMANFIS and ASS with the optimal PID controller to evaluate their performances.

### 4.1. Under ideal conditions

Fig. 7 and Fig. 8 show the simulation results. As can be seen from the Fig. 8, in uncontrolled passive system the vertical sprung mass displacement has significant fluctuations during the whole simulation time so that the maximum overshoot is close to 100% which causes severe vibrations that negatively impact on passengers' health. However, the proposed optimized BBO-FCMANFIS controller has better performance over the passive system and the optimal LQR-PID controller in terms of reducing actuator power consumption and the suppression of the vibration of the sprung mass acceleration, and as a result riding comfort.

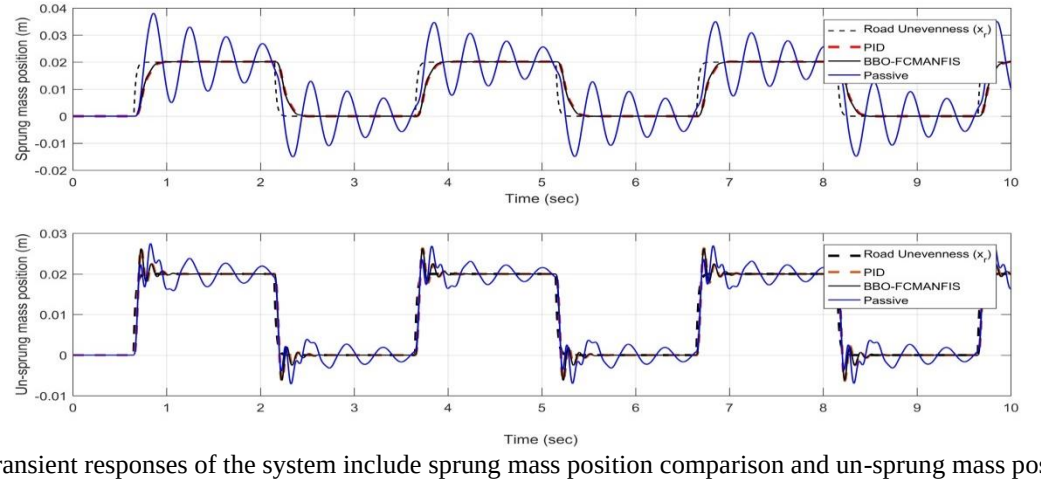


**Fig. 7.** Transient responses of the system include sprung mass position comparison and un-sprung mass position comparison.

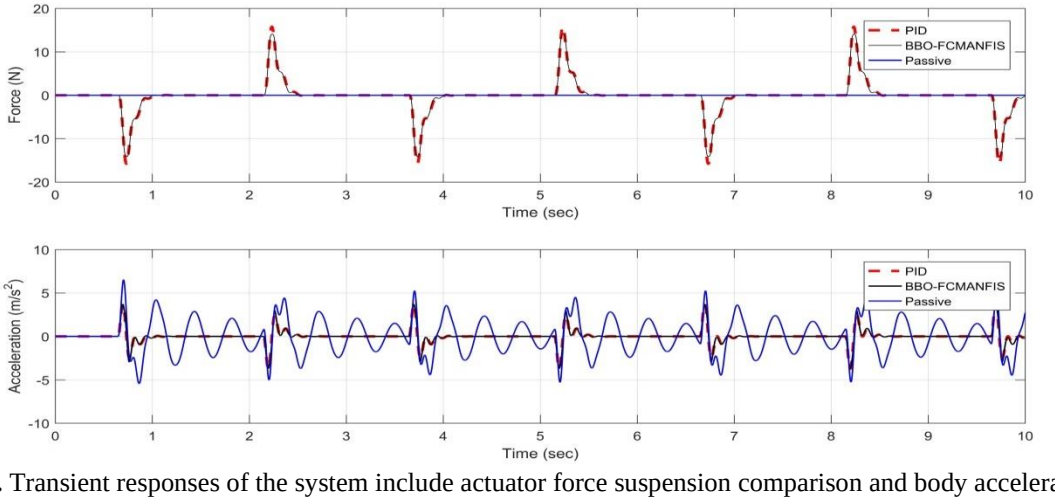


**Fig. 8.** Transient responses of the system include actuator force suspension comparison and body acceleration comparison.

### 4.2. Under parameters' uncertainties

Next, the impacts of variations in system model parameters such as the sprung mass (m_s), suspension stiffness (k_s), and damping coefficient of damper (b_s) on the system response is evaluated. Thus, the sprung mass was increased to 5.5 (kg); suspension stiffness and damper were decreased to 800 (N/m) and 5.5 ((N.s)/m), respectively. The other remaining parameters of the system was assumed unchanged. To evaluate the robustness of the proposed BBO-FCMANFIS controller, this modified model was used to perform simulations. The results were very similar to those was obtained in Fig. 7 and Fig. 8 with a very slight difference, which demonstrates successful model fitting.

### 4.3. Simulation results with actual road data

Power Spectral Density (PSD) values are commonly used for the classification of road unevenness [37]. The real road data like a standard normal distribution with standard deviation 2 (cm) as depicted in Fig. 9.

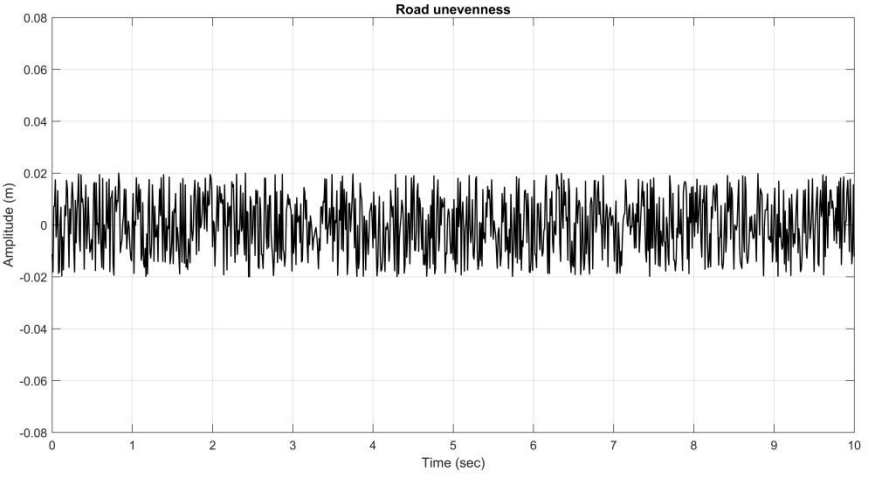


**Fig. 9.** Road input unevenness.

The simulation results are shown in Fig. 10 and Fig. 11. To evaluate the effectiveness of the proposed BBO-FCMANFIS controller, the RMS values of the four variables of ASS were calculated as depicted in Table 2. As it can be seen from these values, the BBO-FCMANFIS uses an average of $0.6547\ (N)$, while the optimal PID controller uses an average of $1.1504\ (N)$. This represents that the BBO-FCMANFIS controller consumes 43% less energy than the optimal PID controller. This energy saving is very important for electric vehicles. Moreover, the vertical acceleration of the sprung mass is the main important parameter that is very effective in passenger comfort. Rapid variations of acceleration are more significant over the variations of displacement or velocity. Thus, it plays main role in minimizing the vertical acceleration of vehicle body. As shown in Fig. 11, the BBO-FCMANFIS controller has better performance as compared with the optimal PID controller in term of suppressing the peaks and the troughs. The obtained RMS values are $0.5167\ (\frac{m}{s^2})$ for the BBO-FCMANFIS controller and $0.5708\ (\frac{m}{s^2})$ for the optimal PID controller which means that the BBO-FCMANFIS controller provide a lower vertical body acceleration over the optimal PID controller with a reduction of 9.5%. Therefore, the presented optimized BBO-FCMANFIS controller has better performance over the optimal LQR-PID controller in the presence of the real road input data in terms of reducing actuator energy consumption and the suppression of the vibration of the sprung mass acceleration, and as a result riding comfort.

**Table 3.** Comparison of two controllers based on the RMS values of the time responses with the real road data.

| Controller | $x_s\ (m)$ | $x_{us}\ (m)$ | $\ddot{x}_s\ (\frac{m}{s^2})$ | $F_a\ (N)$ |
|---|---|---|---|---|
| Passive | 0.0031 | 0.0115 | 0.8786 | 0 |
| PID | 0.0027 | 0.0114 | 0.5708 | 1.1504 |
| BBO-FCMANFIS | 0.0025 | 0.0102 | 0.5167 | 0.6547 |

The PSD of the body acceleration is used to evaluate the quality of vehicle ride which is depicted in Fig. 12 for passive, PID, BBO-FCMANFIS based ASS under the road disturbance input data. As it can be seen from Fig. 12, the acceleration of sprung mass is suppressed by two controllers in the lower frequency band, approximately between $0.4\ (Hz)$ to $9\ (Hz)$. Thus, the proposed BBO-FCMANFIS has good

performance in counter with the road disturbance profile.

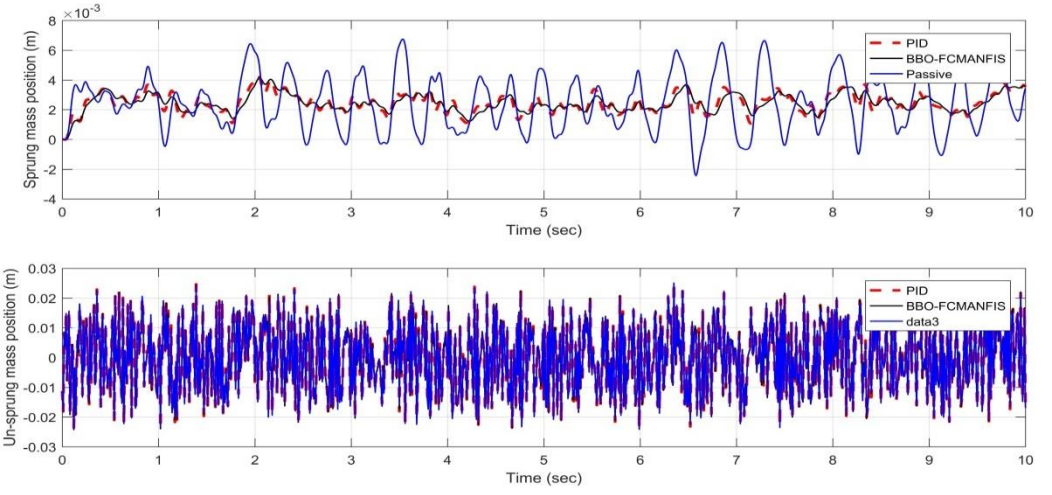


**Fig. 10.** Transient responses of the closed loop suspension system include sprung mass position comparison and un-sprung mass position comparison with actual road data.

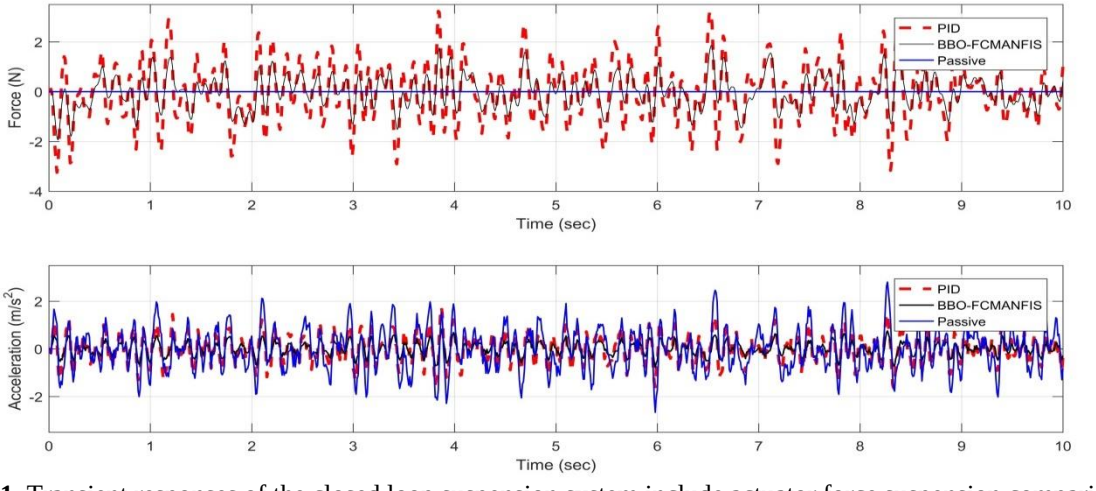


**Fig. 11.** Transient responses of the closed loop suspension system include actuator force suspension comparison and body acceleration comparison.

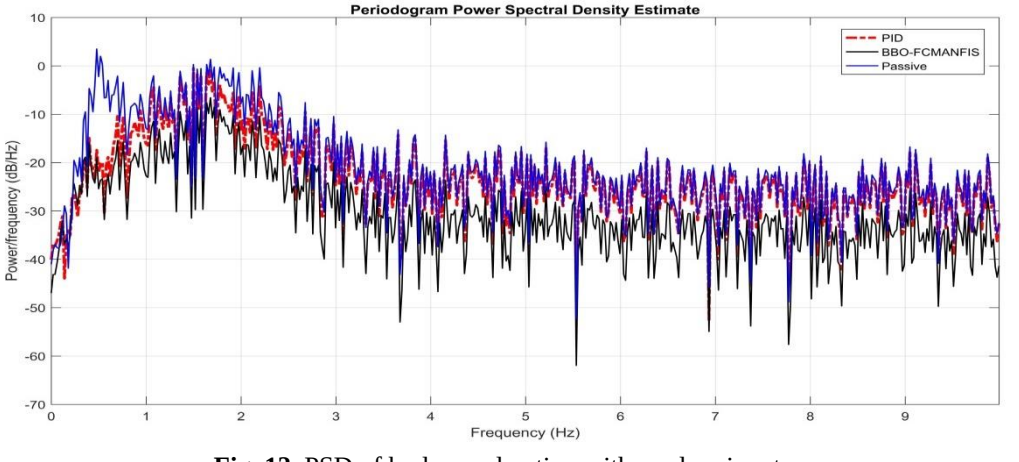


**Fig. 12.** PSD of body acceleration with random input.

## 5. CONCLUSION

In this research an optimum network structure based on a BBO tuned ANFIS was proposed to improve the performance of an ASS. To illustrate the efficiency and the robustness of the proposed control strategy, real-time simulation was conducted in MATLAB/Simulink. Simulation results illustrate that the proposed BBO-FCMANFIS outperforms the optimal PID controller in both ideal and uncertainties conditions. Moreover, simulation was performed with actual road profiles. Simulation results show that the proposed BBO-FCMANFIS controller has lower energy consumption than the optimal PID controller with a reduction of 43% which is significant and very important for electric vehicles. Besides, The proposed BBO-FCMANFIS controller provide a lower overall body acceleration over the optimal PID controller with a reduction of 9.5% which positively impact on the safety, health, and comfort of passengers.

## REFERENCES


[1] M. M. Elmadany, A. EI-Tamimi, **"On a subclass of nonlinear passive and sear-active damping for vibration isolation, "** *Comput Struct*, vol. 36, pp. 921-931, 1990.

[2] M. Geravand and N. Aghakhani, **"Fuzzy sliding mode control for applying to active vehicle suspentions, "** *WSEAS Trans Syst Control*, vol. 5, pp. 48-57, 2007.

[3] W. Sun, J. Li, Y. Zhao, and H. Gao, **"Vibration control for active seat suspension systems via dynamic output feedback with limited frequency characteristic, "** *Mechatronics*, vol. 21, pp. 250-260, 2010.

[4] M. Senthil kumar, **"Genetic algorithm-based proportional derivative controller for the development of active suspension system**," *Inf Technol Control*, vol. 36, pp. 58-67, 2007.

[5] G. Priyandoko, M. Mailah, and H. Jamaluddin,**"Vehicle active suspension system using skyhook adaptive neuro-active force control, "** *Mech Syst Signal Process*, vol. 23, pp. 855-868, 2009.

[6] S. Kumar, K. P. S. Rana, J. Kumar et al., **"Self-tuned robust fractional order fuzzy PD controller for uncertain and nonlinear active suspension system, "** *Neural Comput & Applic*, vol. 30, pp. 1827-1843, 2018.

[7] A. A. Aldair, E. B. Alsaedee, and T.Y. Abdalla, **"**"**Design of ABCF Control Scheme for Full Vehicle Nonlinear Active Suspension System with Passenger Seat, "** *Iran J Sci Technol Trans Electr Eng*, vol. 43, pp. 289-302, 2019.

[8] J. Mrazguaa, E. Houssaine-Tisssira, and M. Ouahi, **"Fuzzy Fault-Tolerant $H^{\infty}$ Control Approach for Nonlinear Active Suspension Systems with Actuator Failure, "** Procedia Comput Sci, vol. 148, pp. 465-474, 2019.

[9] J. Na, Y. Huang, X. Wu et al., **"Adaptive Finite-Time Fuzzy Control of Nonlinear Active Suspension Systems With Input Delay, "** *IEEE Trans Cybern*, vol. 50, pp. 2639–2650, 2019.

[10] Y. Qin, J.J. Rath, C. Hu et al., **"Adaptive nonlinear active suspension control based on a robust road classifier with a modified super-twisting algorithm, "** *Nonlinear Dyn*, vol. 97, pp. 425-2442, 2019.

[11] D. Singh, **"Modeling and control of passenger body vibrations in active quarter car system: a hybrid ANFIS PID approach, "** *Int J Dynam Control*, vol. 6, pp. 1649-1662, 2018.

[12] D. Singh, **"Whole body active vibration control of passenger biodynamics in quarter car model under random road excitations using ANFIS gain tuned PID-super twisting control, "** *Int J Dynam. Control*, vol. 8, pp.999–1012, 2020.

[13] Q. Wang, Y. Zhao, H. Xu et al., **"Adaptive backstepping control with grey signal predictor for nonlinear active suspension system matching mechanical elastic wheel, "** *Mech Syst Signal Process*, vol. 131, pp. 97-111, 2019.

[14] S. Liu, T. Zheng, D. Zhao et al., **"Strongly perturbed sliding mode adaptive control of vehicle active suspension system considering actuator nonlinearity, "** *Veh Syst Dyn* (2020), 10.1080/00423114.2020.1840598

[15] Sy. Dzung Nguyen, B. Danh-Lam, S.B. Choi, **"Smart dampers-based vibration control -Part 2: Fractional order sliding control for vehicle suspension system,"** *Mech Syst Signal Process*, vol. 148, (2021), https://doi.org/10.1016/j.ymssp.2020.107145

[16] [16] P. Swethamarai, P. Lakshmi,**"** "**Adaptive-fuzzy fractional order PID controller-based active suspension for vibration control,"** *IETE J Res* (2020), https://doi.org/10.1080/03772063.2020.1768906

[17] M. J. Mahmoodabadi and N. Nejadkourki, "**Optimal fuzzy adaptive robust PID control for an active suspension system**," *Aust J Mech Eng* (2020), https://doi.org/10.1080/14484846.2020.1734154

[18] H. Pang, X. Zhang, Z. Xu, **"Adaptive backstepping-based tracking control design for nonlinear active suspension system with parameter uncertainties and safety constraints,"** *ISA Trans*, vol. 88, pp. 23-36, 2019.

[19] Y. Kuo and T. Li, **"GA based Fuzzy PI/PD controller for automotive active suspension system,"** *IEEE Trans Ind Electron*, vol. 46, pp.1051-1056, 1999.

[20] J. Feng and F. Yu, **"GA-based PID and fuzzy logic controller for active vehicle suspension system,"** *Int J Automot Technol*, vol. 4, pp. 181-191, 2003.

[21] J. S. Lin and I. Kanellakopoulos, **"Nonlinear design of active suspension,"** *IEEE Control Syst*, vol. 17, pp. 45-59, 1997.

[22] C. Kim and P. I. Ro, **"**A **sliding mode controller for vehicle active suspension systems with nonlinearities,"** *Proc IMechE Part D: J Autom. Eng*, vol. 212, pp. 79-92, 1998.

[23] T. Yoshimura, A. Kume, M. Kurimoto, et al.,**"Construction of an active suspension system of a quarter car model using the concept of sliding mode control,"** *J Sound Vib*, vol. 239, pp. 187-199,

2001.

[24] S. J. Huang and W. C. Lin, **"Adaptive fuzzy controller with sliding surface for vehicle suspension control,"** *IEEE Trans Fuzzy Syst*, vol. 11, pp. 550-559, 2003.

[25] J. Lin, R. J. Lian, C. N. Huang, , et al., **"Enhanced fuzzy sliding mode controller for active suspension systems,"** *Mechatronics*, vol. 19, pp. 1178-1190, 2009.

[26] S. J. Huang and W. C. Lin, **"A neural network based sliding mode controller for active vehicle suspension,"** *Proc IMechE Part D: J Autom Eng*, vol. 221, pp. 1381-1397, 2007.

[27] F. J . D'Amato and D. E. Viassolo, **"Fuzzy control for active suspensions, "** *Mechatronics*, vol. 10, pp. 897-920, 2000.

[28] I. Eski and S. Yıldırım, **"Vibration control of vehicle active suspension system using a new robust neural network control system,"** *Simulat Model Pract Theor*, vol. 17, pp. 778-793, 2009.

[29] A. Konoiko, A. Kadhem, I. Saiful, et al., "**Deep learning framework for controlling an active suspension system,"** *J Vib Control*, vol. 25, pp. 2316-2329, 2019.

[30] Y. Zhang and A. Kandel "**Compensatory neurofuzzy systems with fast learning algorithms**," *IEEE Trans Neural Netw Syst* vol. 9, pp. 80-105, 1998.

[31] A .A. Aldair, W. J. Wang, **"Design an intelligent controller for full vehicle nonlinear active suspension systems, "** *Int J Smart Sens Intell Syst*, vol. 4, pp. 224-243, 2011.

[32] R. Kothandaraman and L. Ponnusamy, "**PSO tuned adaptive neuro-fuzzy controller for vehicle suspension systems, "** *J Adv Info*, vol. 3, pp. 57-63 , 2011.

[33] R. Kalaivani and P. Lakshmi, **"Adaptive neuro-fuzzy controller for vehicle suspension system, "** *in Proc. 2013 IEEE International Conference on Advanced Computing (ICAC)*, Chennai, India, 18-20 Dec. 2013.

[34] U. Rashid, M. Jamil, and S. Gilani, **"LQR based training of adaptive neuro-fuzzy controller, "** *J Intell Fuzzy Syst*, vol. 54, pp. 311-322 ,2016.

[35] M. Cui, L. Geng, and Z. Wu, **"Random Modeling and Control of Nonlinear Active Suspension**," *Math Probl Eng*, (2017), https://doi.org/10.1155/2017/4045796

[36] S. Yan, E. L. Dowell, and B. Lin, **"Effects of nonlinear damping suspension on nonperiodic motions of a flexible rotor in journal bearings,"** *Nonlinear Dyn*, vol. 78, pp. 1435–1450 ,2014.

[37] G.D. Nusantoro and G. Priyandoko, **"PID state feedback controller of a quarter car active suspension system,"** *J Basic Appl Sci Res*, vol. 1, pp. 2304-2307, 1994.

[38] D. Simon, **"Biogeography based optimization, "** *IEEE Trans Evol Comput*, vol. 12, pp. 702-713, 2008